

Stabilization of Expansive Black Cotton Soil using Alkali Activated Binder with Glass and Polypropylene Fiber

Mazhar Syed¹[0000-0002-0728-9148], Sagar Agarwal¹, and Anasua GuhaRay^{1*}[0000-0002-4973-0499]

¹ BITS-Pilani Hyderabad Campus, Telangana, India 500078.
p20170007@hyderabad.bits-pilani.ac.in; f20160447@hyderabad.bits-pilani.ac.in;
guharay@hyderabad.bits-pilani.ac.in

Abstract. Expansive soil exhibit high swelling and shrinkage behavior when moisture fluctuation occurs, this volumetric variation in black cotton soil (BCS) renders unsuitable for use in geotechnical applications. The present paper emphasizes an experimental investigation on the effect of discrete polypropylene (PP) and glass fiber (GF) with alkali activated binder (AAB) on geomechanical properties of BCS. Hence the present study aims to compare the geoen지니어ing and microstructural characteristics between PP and glass fiber on AAB treated BCS. PP and GF were varied from 0 to 0.4% with 5% AAB in the BCS. AAB is produced by the reaction between alkali activator solution (sodium hydroxide and sodium silicate) and aluminosilicate precursor (Class-F fly ash/slag). Microstructural analysis for AAB treated BCS reinforced with both PP and GF are performed through a stereomicroscope, X-ray diffraction (XRD), Fourier-transform infrared spectroscopy (FTIR), scanning electron microscope (SEM), and energy dispersive x-ray spectroscopy (EDS). The unconfined compressive strength (UCS), indirect tensile strength (ITS) California Bearing Ratio (CBR) and linear shrinkage tests for glass fiber-AAB and PP fiber-AAB treated BCS are carried out. The influences of varying percentages of different fiber with AAB content in the BCS show a significant improvement in geoen지니어ing properties especially tensile strength. It is observed that the addition of 5% AAB with 0.3% of glass fiber and PP fiber reduces the linear shrinkage by 12-15% while CBR and ITS values are increased by 20-30%. From the results, it is observed that the PP fiber-AAB treated BCS achieve maximum mechanical strength when compares to glass fiber-AAB treated BCS.

Keywords: Black Cotton Soil, Alkali Activated Binder, Polypropylene and Glass Fibers, Geoen지니어ing Characteristics, Microstructural Analysis.

1 Introduction

Expansive black cotton soil (BCS) has a low volumetric stability due to a high concentration of montmorillonite and smectite group, which increase the swelling and shrinkage characteristics during wetting and drying season [1, 2]. Chemical soil stabilization by lime and cement is an effective method to upgrade the geomechanical characteristics of these expansive soils by altering physico-mechanical behavior [3,

4]. However, the production of this calcium-based binder has shown a great impact on the environment by releasing carbon dioxide and greenhouse gases [5, 6]. Hence it is always encouraged to utilize the industrial by-products such as fly ash [7,8], agro-waste like palm oil fuel ash, rice husk ash, cement kiln dust, solid wastes like Ground Granulated Blast Furnace Slag (GGBS), bagasse and volcanic ash [9-10], as full or partial replacement with conventional cementitious binders along with inclusion of geotextiles, fibers [11, 12]. Disposal of these industrial by-products is a serious issue. In India, power plant produces nearly 95 million tons of fly ash per annum as per IRC-SP-20-2002 and almost 85% of ash produced is very fine in nature. Therefore, the utilization fly ash/slag with cementitious binder aids to serve the dual benefits of improving the soil bearing capacity and preventing the disposal into dumping yard [8, 9, 10]. Multiple research is carried out to improve the geomechanical behavior in terms of tensile and shear strength of soil with a combination of cementitious binder and fiber [11, 12]. However, limited studies are reported on the comparison of tensile strength using AAB as an additive to soil, reinforced with glass and polypropylene fiber.

The present study aims to utilize the industrial by-product precursors with low carbon emission binder as a cementitious additive for ground improvement. The study proposes a method of geopolymerisation of expansive black cotton soil by blending Class-F fly ash with a solution of sodium silicate and sodium hydroxide. This mixture combination leads to the formation of alkali-activated binders (AABs) which possess similar mechanical characteristics as hardened cement binder [13, 14]. As a result, their geomechanical properties are also expected to be similar to Portland cement (PC) binder influence. The primary objective of this paper is to improve and compare the tensile strength and ductility behavior of BCS by adding AAB with discrete glass and polypropylene fibers. A series of geotechnical characterization tests are conducted using different percentages of glass and polypropylene fiber with AAB. In addition, microstructural characterizations are also carried out to understand the interfacial mechanism of fiber reinforced AAB treated soil.

2 Material Characteristics

2.1 Expansive black cotton soil (BCS)

BCS used in the present study is collected from Nalgonda district of Telangana state. The soil is dark brown in color and is excavated at 30 cm depth from natural ground surfaces to avoid grabbing of roots. BCS is classified as high plasticity clay (CH) as per Unified Soil Classification System (USCS). The different physical and engineering properties of raw BCS are provided in Table 1. The particle size distribution curves of BCS, along with fly ash are shown in Fig.1. The BCS is sun-dried and ground prior to all the tests.

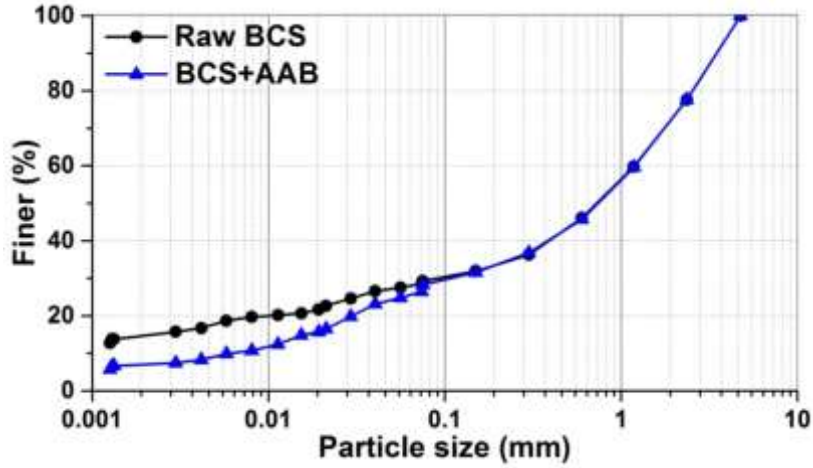


Fig. 1. Particle size distribution curve of raw BCS and AAB treated BCS

Table 1. Engineering properties of raw BCS

Soil Properties	Values
Specific Gravity	2.59
Optimum Moisture Content, OMC (%)	24.5
Maximum Dry Density, MDD (g/cc)	1.65
Liquid Limit, LL (%)	62.0
Plasticity Index, PI (%)	38.0
Free Swelling Index, FSI (%)	86.0
Indirect Tensile Strength, ITS (kPa)	12.54
Unconfined Compressive Strength, UCS (kPa)	185
California Bearing Ratio, CBR (%) Soaked	1.96

2.2 Polypropylene (PP) and Glass fiber (GF)

Polypropylene and Glass fiber used in this study are acquired by Kankadurga Industries Pvt. Ltd., Hyderabad. Both fibers length of 12 mm is adopted for all the tests. Fig. 2 shows the physical appearance of both polypropylene and glass fiber.



Fig. 2. Image showing discrete Polypropylene and Glass fiber

2.3 Alkali activated binder (AAB)

AAB is prepared by mixing sodium silicate solution with crushed sodium hydroxide pellets and water with fly ash, by maintaining the mass ratio of sodium hydroxide to sodium silicate to fly ash is 10.57:129.43:400 [12]. The sodium silicate solution and sodium hydroxide pellets are obtained from HYCHEM Chemical Laboratories. Fly ash is obtained from NTPC thermal power plant Ramagundam.

2.4 Preparation of Soil Sample

BCS is uniformly mixed with 5% of AAB paste (total mass of soil) by maintaining 0.4 w/s ratio in the AAB compound. AAB mixed soil is compacted in three layers with a 9 kg steel rammer falling freely from a height of 310 mm. The compacted soil is covered with moist jute bags for 24 hours. Prior to random mixing of different percentages (0%, 0.1%, 0.2%, 0.3%, and 0.4% mass of BCS) of GF and PPF in the AAB soil.

Results and Discussion

2.5 Microstructural Characterization

X-ray diffraction (XRD). Powder X-ray diffraction analyses are performed to identify the mineral crystallinity present in untreated BCS, glass and polypropylene fiber reinforced AAB treated BCS using a RIGAKU Ultime IV diffractometer with CuK α rays generated at 40 mA and 40 kV by operating 2 θ ranges from 00 to 800 with a step 0.020 for 2 θ values at 2 seconds per step. Fig. 3 shows the XRD pattern of BCS. Raw BCS reveals the presence of clay minerals such as Montmorillonite (M), Quartz, (Q) and Muscovite (Ms) [12]. Further addition of fly ash based sodium aluminosilicate binder in BCS with fibers shows the additional peaks corresponding to Mullite (Mu) and Augite (Au), which are characteristic of hardened AAB paste. Moreover, the XRD pattern of both glass and polypropylene fiber reinforced AAB soil shows the negligible changes between the peak intensities, as is evident from the diffractograms. The formation of new minerals in the BCS may be attributed to the geopolymerization reaction of AAB. Hence it can be concluded that both the fibers in AAB will remain in conjunction with BCS after forming.

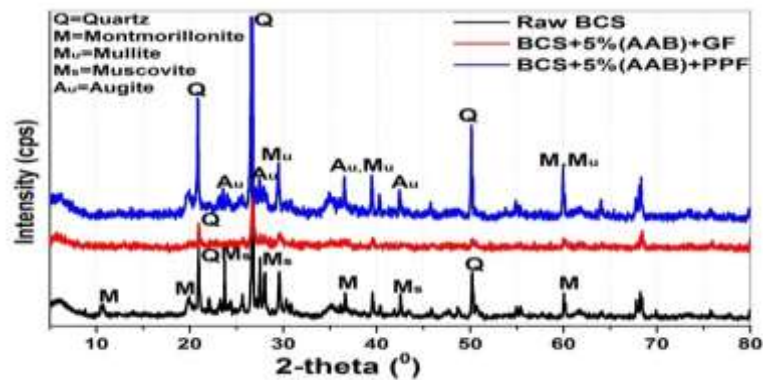


Fig. 3. Xrd pattern of untreated BCS and fiber-AAB treated BCS

Fourier transfer infrared (FTIR) spectroscopy. Fourier-transform infrared (FTIR) spectroscopy is conducted to analyze the molecular bonding vibration present in untreated BCS, glass and polypropylene fiber reinforced AAB treated BCS using a JASCO FTIR 4200 setup through KBr pellet arrangement between 4000-500 cm^{-1} infrared spectroscopy. Fig 4 shows the transmittance spectrum curves of untreated and fiber-AAB treated BCS. Raw BCS shows O-H stretching vibrations around 3615 cm^{-1} , which is the general characteristic of montmorillonite. AAB treated BCS shows slight reduction in the intensity of chemical bonds corresponding to montmorillonite. Furthermore, the broadband is found at 3450 cm^{-1} corresponding to O-H stretching of the hydroxyl group. C=O carbonyl bond is also detected at 1730 cm^{-1} for all samples. Another main peak at 1033 cm^{-1} , 785 cm^{-1} and 527 cm^{-1} are attributed to Si-O-Si, Al-

O. Si-O-Al bonds are visible in raw and fiber-AAB BCS samples, but most of them show a chemical shift of about 10 cm^{-1} .

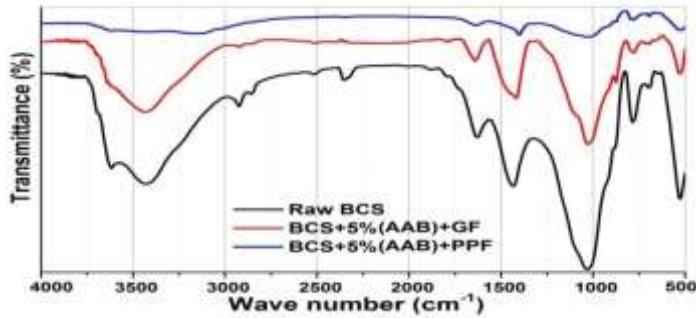
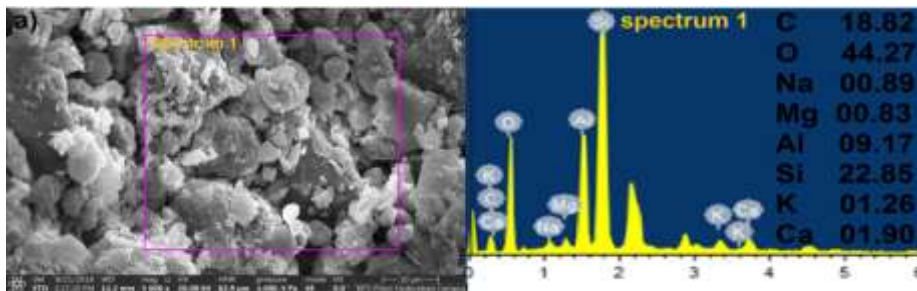


Fig. 4. FTIR spectroscopy of untreated BCS and fiber-AAB treated BCS

Scanning electron microscope (SEM) and energy dispersive x-ray spectroscopy (EDX). Soil surface micrographs and elemental compositions of untreated BCS, glass and polypropylene fiber reinforced AAB treated BCS are examined using a Thermo Scientific Apreo SEM provided by FEI (Field Electron and Ion Company) at different magnifications and spot regions. Energy dispersive x-ray spectra (EDS) are recorded using Aztec analyzer system provided by Oxford Instruments with a probe current of $65\ \mu\text{A}$ at a working distance of 10mm. Fig. 5a shows the morphology of untreated BCS, which reveals the flocculated flaky microstructure, In addition, Oxygen (O) and silica (Si) are found to be the major components. Fig. 5b and 5c show the micrographs of discrete polypropylene and glass fiber matrix incorporated with fly ash based AAB paste around the aggregated clayey surfaces. This fiber-AAB mixture acts as spatial thread groove network by interlocking the clayey particles through bonding. Moreover, the peak intensities of Silica (Si), and Calcium (Ca) become relatively stronger in AAB treated BCS.



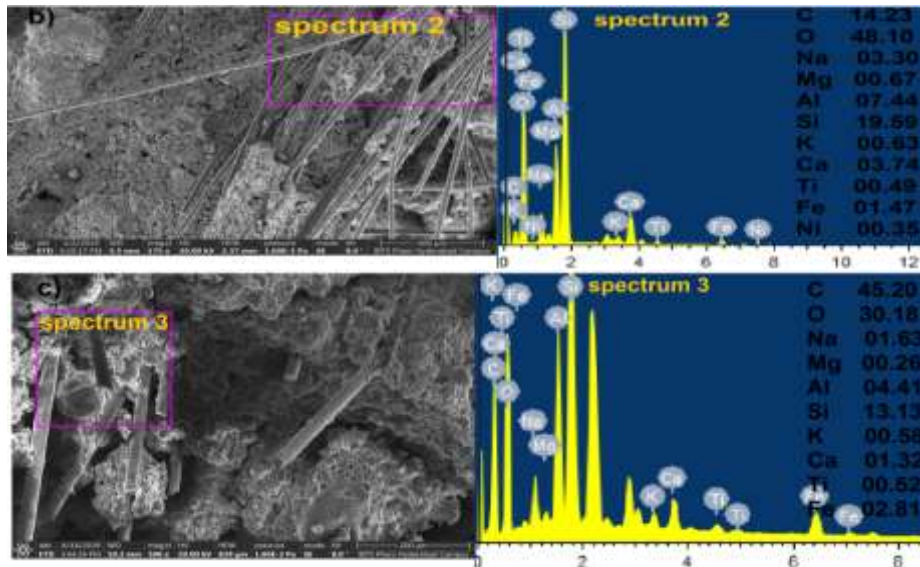


Fig. 5. SEM/EDS images of (a) Untreated BCS (b) Polypropylene fiber reinforced AAB treated BCS (c) Glass fiber reinforced AAB treated BCS.

Stereomicroscopic Images. Stereomicroscopic images are used to visualize the surface images of untreated BCS, glass and polypropylene fiber reinforced AAB treated BCS using an Olympus SXZ7 setup with the least dimension of 20 μm . Fig. 6a shows the surface images of untreated BCS, which consist of light red colour particles with some brown regions, indicating the presence of iron, illite and smectite group [4, 12]. Fig. 6b shows the deposition of hardened AAB paste with polypropylene fiber around the BCS. Fig. 6c shows the discrete glass fiber matrix embedded in AAB treated BCS, which act as bonding bridge network between the particles.



Fig. 6. Stereomicroscopy images of (a) Untreated BCS (b) Polypropylene fiber reinforced AAB treated BCS (c) Glass fiber reinforced AAB treated BCS.

2.6 Geotechnical Characterization

Detailed geotechnical characterization is performed using compaction, shear, tensile resistance, consolidation and California bearing ratio tests for both untreated BCS and fiber reinforced AAB treated BCS. All the soil specimens are prepared with respect to their MDD and OMC values. These experimental results are used to assess the effectiveness of binder and mechanical behavior of fiber reinforced-AAB-treated BCS. The details of the tests and the discussion of test results are given in the following sections.

Compaction. A series of standard Proctor compaction tests are performed as per ASTM D-698 standard for untreated BCS, glass and polypropylene fiber reinforced AAB treated BCS (Fig. 7). MDD and OMC of raw BCS are found 1.65 g/cc and 24.5%. The intrusion of fly ash based sodium aluminosilicate binder increases the MDD value from 1.65 to 1.82 g/cc, mainly fiber-AAB attributes towards the filling of voids between the clayey particles and reduction of specific surface area in the soil [3]. It is also interesting to note that the optimum moisture content of AAB modified BCS reduces from 24.5 to 18.6%. This reduction may be because of induced pozzolanic reaction and flocculation mechanism due to encapsulation of clayey particles by deposition of hardened AAB paste with fiber matrix. The increase in MDD and decrease in OMC is an indicator of improving the shear strength properties of soil.

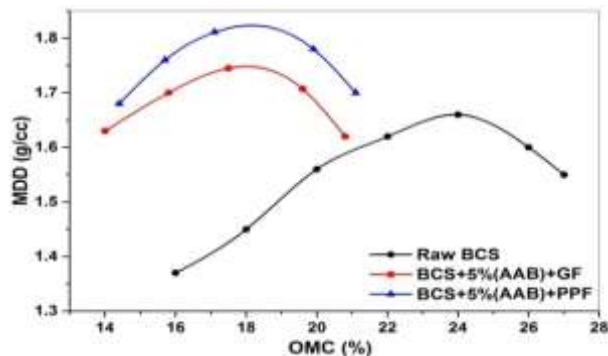


Fig. 7. Variation of MDD and OMC values of untreated BCS and fiber-AAB treated BCS

Linear shrinkage. The linear shrinkage tests are carried out as per the Australian AS1289-C4 standard code for both untreated BCS and fiber reinforced AAB treated BCS. Fig. 8 shows the variation of shrinkage value with respect to fiber content. The shrinkage limit and linear shrinkage of raw BC are 15.3% and 26.8% respectively. The addition of AAB in BCS leads to reduce the shrinkage properties. Further addition of fiber in the AAB modified BCS shows a marginal effect on linear shrinkage and controls the cracks effectively. This reduction may be attributed towards the formation of pozzolanic phenomena around the clay surfaces [4, 15].

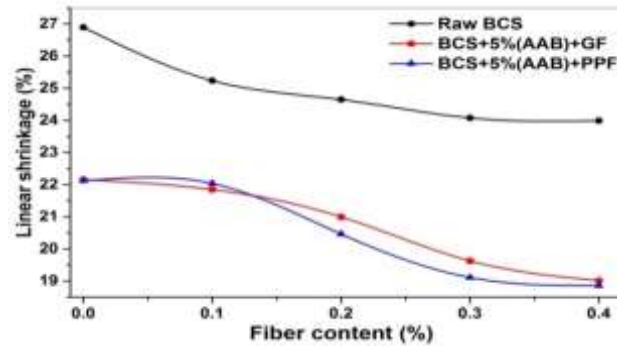


Fig. 8. Variations of linear shrinkage values of untreated BCS and fiber-AAB treated BCS

Consolidation and Swelling Pressure. Consolidation and swelling pressure tests are conducted in an Oedometer according to ASTM D-2435 and D-4546 standards. Both untreated BCS, as well as fiber-AAB treated BCS samples, are statically compacted at MDD and OMC in a consolidation ring of 20 mm height and 60 mm diameter. Fig. 9a shows the slope of compressibility curve of treated and untreated BCS. In the e -log p curve of consolidation, raw BCS attains the highest equilibrium void ratio and the polypropylene fiber-AAB treated BCS attains least void ratio on saturation. However, the inclusion of glass fiber in the AAB treated BCS does not significantly alter the void ratio when compared to polypropylene fiber-AAB treated BCS. Fig.9b shows the time swell curve of untreated BCS, glass and polypropylene fiber reinforced AAB treated BCS. Raw BCS has the maximum swelling pressure of 78 kPa; both fiber-AAB mixtures blended soil attains maximum swelling pressure around 39kPa. This reduction of swelling may be due to the formation of new mineralogy by dissolution of clay particles with pozzolanic additives [16, 17].

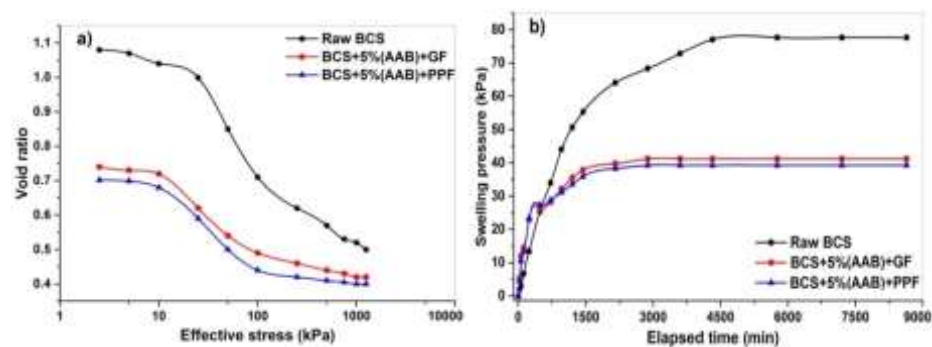


Fig. 9. Variation of (a) e -log (p) curves (b) Swelling pressure of untreated BCS and fiber-AAB treated BCS

Indirect tensile strength (ITS). Indirect tensile tests are conducted as per ASTM D4123-1995 standard on both untreated and AAB treated BCS with different fibers.

The soil specimens are prepared by maintaining 80 mm height and 100 mm diameter with a loading strip of 12.5mm at a constant strain rate of 50.5mm/min in a Marshall Stability machine. The samples are preserved for 24 hours in the humidity chamber before testing. Fig. 10a shows the tensile strength of soil with respect to fiber. Addition of glass and polypropylene fibers in the AAB treated BCS increases the tensile resistance strength from 24 to 190 kPa. Thus the enhancement in ductile behavior of BCS may be because of the fiber surface morphology and pozzolanic reaction induced in the clay bonding. Fig. 10b shows the typical arrangement of indirect tensile strength test of soil under the loading strip frame.

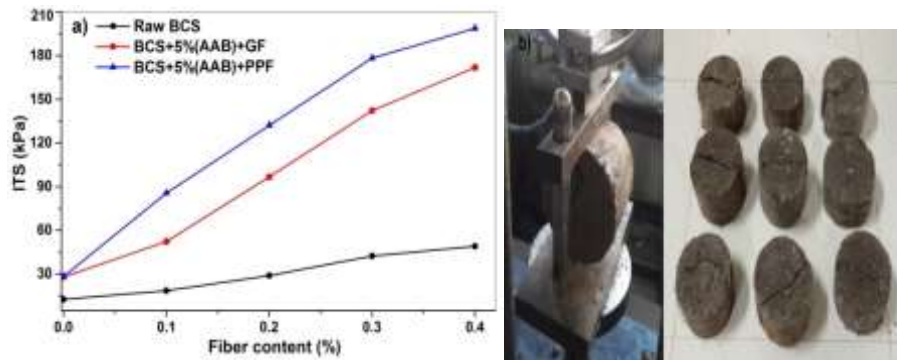


Fig. 10. Variation of ITS values of untreated BCS and fiber-AAB treated BCS (b) Typical arrangement of ITS test

Unconfined compressive strength (UCS). Unconfined compressive strength tests are performed for untreated BCS, glass and polypropylene fiber reinforced AAB treated BCS as per ASTM D-2166 standard. Soil samples are molded in 38 mm diameter and 76 mm molds at MDD and OMC values under a fixed strain rate of 1.25 mm/min. Fig. 11a shows the shear strength values of soil with respect to fiber. Combined addition of glass or polypropylene fibers in the treated BCS shows relatively higher shear resistance. This abrupt enhancement in shear strength may be attributed to the formation of interfacial friction and confinement bonding between the fiber and clay particles. Fig 11b shows the stress-strain curve of treated and untreated BCS. Thus the inclusion of polypropylene fiber in AAB modified soil attains maximum compressive strength when compared to glass fiber-AAB treated soil.

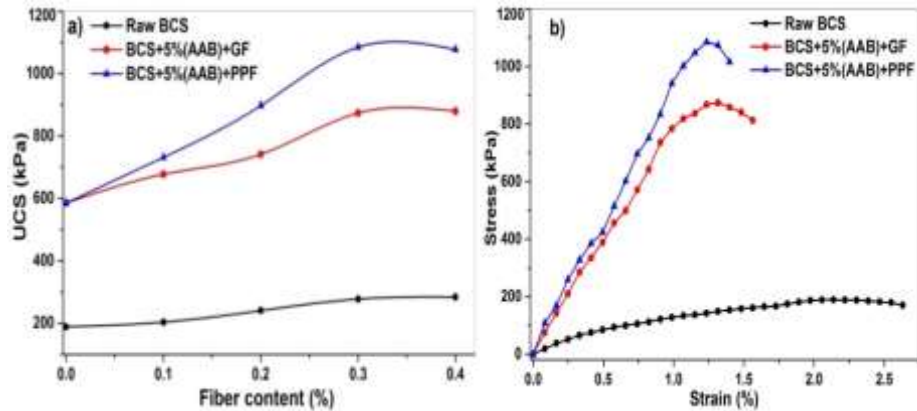


Fig. 11. (a) Variation of UCS with fiber content, (b) Stress-strain curves of untreated BCS and fiber-AAB treated BCS

California bearing ratio (CBR). Soaked and unsoaked CBR tests are performed for untreated BCS, glass and polypropylene fiber reinforced AAB treated BCS, as per ASTM D-1883 standard. Fig. 12 shows the variations of soaked and unsoaked CBR values at 2.5 mm. The soaked CBR value of raw BCS is 1.96, indicating low strength. As seen from the graph, the inclusion of fly ash based sodium aluminosilicate binder with discrete fiber matrix increases the soaked CBR value from 1.96 to 5.59%. This improvement in strength bearing ratio may be because of fiber bonding and pozzolanic reactions.

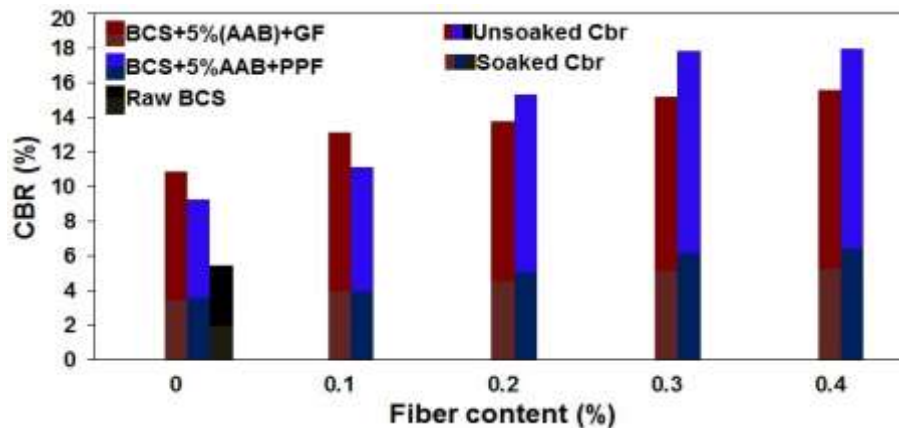


Fig. 12. Variation of soaked and unsoaked CBR values of untreated BCS and fiber-AAB treated BCS

3 Conclusions

The present study compares the geotechnical and microstructure properties of untreated BCS, glass, polypropylene fiber reinforced with envirosafe alkali-activated binders (AAB). Fly ash based sodium aluminosilicate binder serves a dual benefit of reducing traditional based cementitious binders and preventing the disposal of industrial by-product through maintaining a green sustainable environment. The main conclusions that can be drawn from this study are as follows.

- The polypropylene fiber reinforced AAB treated BCS attains higher strength in terms of tensile, bearing capacity and shear resistance when compared to glass fiber- AAB treated BCS.
- Liner shrinkage, void ratio and swelling pressure of fiber AAB treated BCS is significantly reduced by around 30%. Blending of 0.3% polypropylene and/or glass fiber in 5% AAB mixture aids to control the tension cracks significantly.
- The tensile strength and CBR of fiber- AAB treated BCS increase by around 63% and 45% respectively, as the fiber content increases from 0 to 0.4%. Fiber-AAB treated BCS micrograph shows a strong interfacial surface interaction between the fiber and soil matrix.
- Microanalysis results confirm the formation of new crystalline phases and molecular vibrations in fiber-AAB treated BCS. In addition, stereomicroscopic images show that the fiber act as a bridge network between the fiber and clay particles and effectively modify the brittleness characteristic through friction and bonding.

References

1. Ackroyd L.W. and Husain R. Residual and lacustrine black cotton soils of north-east Nigeria. *Geotechnique*. Vol. 36(1) (1986).
2. Ola S.A. The geology and geotechnical properties of the black cotton soils of northeastern Nigeria. *Engineering Geology*. Vol 12, pp. 375-391 (1978).
3. Katti R.K. Search for solutions to problems in black cotton soils. Indian Institute of Technology, Bombay (1978).
4. Das B.M. Chemical and mechanical stabilization. Transportation Research Board (2003).
5. Gartner E. Industrially interesting approaches to 'low-CO₂' cements. *Cement and Concrete Research*. Vol. 34(9) (2004).
6. Ouhadi V.R. and Yong N.R. Ettringite formation and behaviour in clayey soils. *Applied Clay Science*. Vol. 42, pp. 258-265 (2008).
7. Lin B., Cerato A.B., Madden A.S. and Elwood Madden M.E. Effect of fly ash on the behavior of expansive soils: microscopic analysis. *Environmental and Engineering Geoscience*, Vol. 19(1), pp. 85-94 (2013).
8. Maneli A., Kupolati W.K., Abiola O.S. and Ndambuki J.M. Influence of fly ash, ground-granulated blast furnace slag and lime on unconfined compressive strength of black cotton soil. *Road Materials and Pavement Design*. Vol. 17(1), pp. 252-260 (2016).

9. Pourakbar S., Asadi A., Huat B.B. and Fasihnikoutalab M.H. Soil stabilisation with alkali-activated agro-waste. *Environmental Geotechnics* (2015).
10. Miao S., Shen Z., Wang X., Luo F., Huang X. and Wei C. Stabilization of Highly Expansive Black Cotton Soils by Means of Geopolymerisation. *Journal of Materials in Civil Engineering*. Vol. 29(10), pp. 04017170 (2017).
11. Tang C., Shi B., Gao W., Chen F. and Cai Y. Strength and mechanical behavior of short polypropylene fiber reinforced and cement stabilized clayey soil. *Geotextiles and Geomembranes*. Vol. 25(3), pp. 194-202 (2007).
12. Gupta S., GuhaRay A., Kar A. and Komaravolu V.P. Performance of alkali-activated binder-treated jute geotextile as reinforcement for subgrade stabilization. *International Journal of Geotechnical Engineering*. pp. 1-15 (2018).
13. Rios S., Cristelo N., Viana da Fonseca A. and Ferreira C. Structural performance of alkali-activated soil ash versus soil cement. *Journal of Materials in Civil Engineering*. Vol. 28(2), pp. 04015125 (2015).
14. Madejova J. and Komadel P. Baseline studies of the clay minerals society source clays: infrared methods. *Clays and clay minerals*. Vol. 49(5), pp. 410-432 (2001).
15. Mishra A.K. and Sridharan A. A critical study on shrinkage behaviour of clays. *International Journal of Geotechnical Engineering*, pp. 1-11 (2017).
16. Zhao H., Louis Petry T. and Yi-Zhen S. Effects of chemical stabilizers on an expansive clay. *Journal of Civil Engineering, KSCE*, Vol. 10, pp. 1-9 (2013).
17. Vitale E., Russo G., Dell'Agli G., Ferone C. and Bartolomeo C. Mechanical Behaviour of Soil Improved by Alkali Activated Binders. *Environments*, Vol. 4(4), pp. 80 (2017).